Dual-Hop Full-Duplex DF Relay Channel with Parallel Hybrid RF/FSO Links

Michalis P. Ninos, Priyadarshi Mukherjee, Constantinos Psomas, and Ioannis Krikidis
IRIDA Research Centre for Communication Technologies
Department of Electrical and Computer Engineering, University of Cyprus
Emails: {ninos.michail, mukherjee.priyadarshi, psomas, krikidis}@ucy.ac.cy

***Abstract*—In this paper, we carry out a performance analysis of a full-duplex (FD) relaying system consisting of parallel hybrid radio frequency (RF)/free-space optical (FSO) communication links. The RF links are hampered by the residual self-interference (RSI), due to the FD relaying operation, along with the in-phase and quadrature-phase imbalance (IQI) effect, due to imperfections at the RF nodes' front-ends. The parallel FSO links, of the dual-hop configuration, are influenced by the joint effects of atmospheric turbulence and pointing errors. The performance of the dual-hop FD system with parallel hybrid RF/FSO links, operating under a hard-switching scheme, is evaluated in terms of the outage probability. Analytical closed-form expressions are derived for both RF and FSO subsystems as well as for the overall dual-hop hybrid system. The presented numerical results show the significant performance gains obtained by the exploitation of parallel RF/FSO links in an FD relaying channel under various operating conditions. Finally, the derived analytical results are verified by Monte Carlo simulations.**

***Index Terms*—Hybrid RF/FSO systems, full-duplex relaying, dual-hop, self-interference, IQ imbalance, atmospheric turbulence, pointing errors, outage probability.**

I. Introduction

As the transmission characteristics of radio frequency (RF) and free-space optical (FSO) communication systems are complementary to each other [1], hybrid RF/FSO systems have been proven very attractive for the implementation of high performance and high availability wireless links [2]. For instance, FSO systems are significantly influenced by fog which causes optical power loss greater than 10 dB/km, whereas an RF link in the microwave band can remain intact [2]. On the other hand, millimeter-wave RF links can be strongly affected by rain, which has a weaker impact on FSO communications. Also, FSO systems are extremely prone to atmospheric turbulence and pointing errors [3], [4], while RF communication systems are subjected to multipath fading [5]. Thus, the combination of a parallel hybrid RF/FSO topology can circumvent all the aforementioned performance barriers, providing high throughput performance, enabled by the FSO technology, while maintaining connectivity in almost every weather condition due to the RF links.

One promising technique for the RF systems is the full-duplex (FD) operation. In-band FD RF systems transmit and receive in the same frequency band simultaneously, thereby offering an exceptional way of using optimally the time and frequency resources [6]. However, FD systems suffer from the inevitable self-interference (SI) due to signal leakage from the transmit to the receive port. Although advanced analog and digital SI cancellation techniques have been developed, residual self-interference (RSI) signal power can still hamper the performance of such systems [7].

In addition, relaying architectures, either with a decode-and-forward (DF) or an amplify-and-forward protocol, are able to preserve high transmission rates while extending the wireless range of the communications systems [5], [8]. A very useful extension of FD operation is its incorporation into relaying architectures [5]. Major performance benefits emerge by the exploitation of FD relaying systems, taking into consideration that conventional RF relay architectures operate in half-duplex (HD) mode, i.e. transmit and receive at different spectral bands or different time slots (orthogonal channels) [9]. In this way, FD relaying offers very high spectral efficiency, where the relay node transmits and receives at the same frequency band simultaneously, at the expense of potential performance deterioration due to RSI [5], [9]. Furthermore, RF systems suffer from hardware imperfections. Specifically, amplitude and phase mismatches between the in-phase (I) and quadrature-phase (Q) paths can arise due to imperfect local oscillators (LO). As a result, an imbalanced baseband signal can be corrupted by its image, thus leading to interference and signal-to-noise ratio (SNR) deterioration, an effect known as IQ imbalance (IQI) [10], [11].

In this context, few works exist in the literature, investigating the parallel hybrid RF/FSO relay channel. In [12], optimal relay selection policies are investigated for the parallel hybrid RF/FSO channel. In [13], a switching-based cooperative DF relaying network with hybrid FSO/RF links and maximal ratio combining at the destination is investigated. Also, a hybrid FSO/RF millimeter waves with serial DF relaying is presented in [14]. Considering the fact that all the aforementioned works take into account HD relaying operation for the RF links, our motivation focuses on the investigation of an FD relaying operation for the RF links, due to their previously mentioned advantageous features. More specifically, we investigate a dual-hop FD DF relaying network, where each hop is composed of parallel hybrid RF/FSO links. The proposed dual-hop FD system operates under the hard-switching scheme [1]. The RF subsystem is influenced by the RSI due to the FD relaying scheme, the IQI effect at the RF front-ends and the Rayleigh

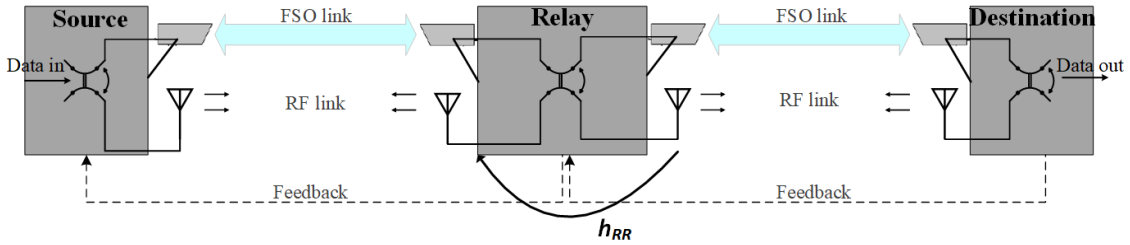

Fig. 1. Block diagram of the considered dual-hop FD DF relay channel with parallel hybrid RF/FSO links under hard-switching operation.

multipath fading. For the FSO links, we take into account beam propagation impairments by the joint effects of atmospheric turbulence and pointing errors. The numerical results present realistic conditions of operation for such FD DF relaying systems with hybrid RF/FSO links and unveil the critical performance characteristics considering the RSI, IQI and Rayleigh fading for the RF subsystem and atmospheric turbulence with pointing errors for the FSO subsystem.

The remainder of this paper is organized as follows. Section II describes the RF and FSO subsystems, where all the effects that influence their performance are considered. Section III presents the closed-form expressions for the outage probability of the individual RF and FSO subsystems as well as of the dual-hop FD hybrid system. Numerical results are presented in Section IV, followed by our conclusions in Section V.

II. System Model

The proposed dual-hop FD communication system consists of a source S, an FD DF relay R, and a destination D. The source S transmits the information symbols by using the RF or the FSO subsystems according to the hard-switching scheme. The hard-switching scheme is based upon the selection combining (SC) criterion [1], [15]. The activation of a subsystem is implemented with the selection of the highest SNR among them, while the other remains idle. At the relay R, the decoded information is forwarded for transmission towards D, by using again a hard-switching scheme. To sum up, at a specific time slot, the subsystems, between the $S-R$ and $R-D$ links, with the highest SNRs are selected for data transmission. Consequently, we present the RF and FSO subsystems.

A. RF Subsystem

For the RF links, of the dual-hop FD system, we employ the standard additive white Gaussian noise (AWGN) model. In addition, we take into account the effect of IQI at the transmitters (TXs) and receivers (RXs) of the RF nodes. The IQ mismatches are almost inevitable in the majority of the RF front-ends and hence, the IQI baseband signal is

$$x^{u/d}_{X,IQI}(t) = K^{u/d}_{1,X} x_X(t) + K^{u/d}_{2,X}(x_X(t))^* \tag{1}$$

with $x_X(t)$ being the desired signal and $(.)^*$ denoting its image. Here we have $K^{u/d}_{1,X}$=$0.5\left(1+\epsilon^{u/d}_X \exp\left(\pm j\phi^{u/d}_X\right)\right)$ and $K^{u/d}_{2,X}$=$1-\left(K^{u/d}_{1,X}\right)^*$ with u/d denoting the up/down-conversion processes and $X \in (R, D)$. Moreover, $\epsilon^{u/d}_X$, $\phi^{u/d}_X$ denote the amplitude and the phase mismatches at the LO signals of the TX/RX of each node. The severity of the IQ mismatches is quantified by the image rejection ratio (IRR) $IRR^{u/d}_X = \left| K^{u/d}_{1,X} / K^{u/d}_{2,X} \right|^2$, whose values, for typical front-end integrated circuits, ranges from 20 to 40 dB [10], [11].

The source S, provided that the RF link is active, transmits a symbol $x_S(t)$ with an average transmitted power $\mathbb{E}[|x_S(t)|^2] = P_t$ which propagates through the Rayleigh block fading channel. At S, we assume that the effect of IQI is handled properly with I/Q pre-compensation schemes [16]. At the relay R, considering front-end imperfections with IQI, the received signal is expressed as

$$\begin{aligned} y_{R,RF}(t) =& K^d_{1,R} h_{SR} x_S(t) + K^d_{2,R}(h_{SR} x_S(t))^* \\ &+ K^d_{1,R} h_{RR} x^u_{R,IQI}(t) + K^d_{2,R}(h_{RR} x^u_{R,IQI}(t))^* \\ &+ K^d_{1,R} n_R(t) + K^d_{2,R}(n_R(t))^*, \end{aligned} \tag{2}$$

where $x^u_{R,IQI}(t)$ is the IQI-impaired transmitted signal from R with an average transmitted power $\mathbb{E}[|x_R(t)|^2] = P_t$ and $n_R(t) \sim \mathcal{CN}(0, \sigma^2_n)$ is the AWGN. The channel coefficients h_w are circularly symmetric complex Gaussian random variables with zero mean and variance σ^2_w, i.e $h_w \sim \mathcal{CN}(0, \sigma^2_w), w \in (SR, RR, RD)$. In order to simplify the notations, we define $\lambda_w \triangleq 2\sigma^2_w$. The received signal at D, considering IQI at the relay TX and the destination RX, is

$$\begin{aligned} y_{D,RF}(t) =& K^d_{1,D} h_{RD} x^u_{R,IQI}(t) + K^d_{2,D}(h_{RD} x^u_{R,IQI}(t))^* \\ &+ K^d_{1,D} n_D(t) + K^d_{2,D}(n_D(t))^*, \end{aligned} \tag{3}$$

with $n_D(t) \sim \mathcal{CN}(0, \sigma^2_n)$. It is important to note that the direct link between S and D is strongly attenuated and communication between them is established only with the aid of the FD relaying scheme [5].

By using (2) and (3), we now proceed with the evaluation of the signal-to-interference-plus-noise ratio (SINR) for the $S-R$ and $R-D$ RF links, i.e. γ_{SR} and γ_{RD}, respectively. Hence, for the $S-R$ RF link, by taking account of the RSI and IQI impairments, the γ_{SR} is formulated as

$$\gamma_{RF,SR} = \frac{|K^d_{1,R} h_{SR}|^2 P_t}{|K^d_{2,R} h_{SR}|^2 P_t + I P_t + \left(|K^d_{1,R}|^2 + |K^d_{2,R}|^2\right)\sigma^2_n}, \tag{4}$$

where

$$I = |K^d_{1,R} K^u_{1,R} h_{RR} + K^d_{2,R}(K^u_{2,R} h_{RR})^*|^2$$

$$+ |K_{1,R}^{d} K_{2,R}^{u} h_{RR} + K_{2,R}^{d} (K_{1,R}^{u} h_{RR})^{*}|^{2}.$$

In case of perfect matching between the IQ branches, the IQI effect becomes negligible, i.e. $K_{1,R}^{u/d} = 1$ and $K_{2,R}^{u/d} = 0$. Hence, we obtain $I = |h_{RR}|^2$ and (4) reduces to $\gamma_{RF,SR} = P_t |h_{SR}|^2 / \left(P_t |h_{RR}|^2 + \sigma_n^2\right)$.

With regards to the $R - D$ RF link, the transmitted IQI-impaired symbol from R reaches D. The demodulation stage at the RX of D is also influenced by the IQI effect. Hence, for the case of TX/RX IQI-impaired nodes [11], the SINR of the $R - D$ RF link is obtained as

$$\gamma_{RF,RD} \approx \frac{|\vartheta_{11}|^2 + |\vartheta_{22}|^2}{|\vartheta_{12}|^2 + |\vartheta_{21}|^2 + \left(|K_{1,D}^{d}|^2 + |K_{2,D}^{d}|^2\right) \frac{1}{\gamma_{id,RD}}}, \tag{5}$$

where $\vartheta_{11}{=}K_{1,D}^{d} K_{1,R}^{u}$, $\vartheta_{12}{=}K_{1,D}^{d} K_{2,R}^{u}$, $\vartheta_{21}{=}K_{2,D}^{d} (K_{1,R}^{u})^{*}$, $\vartheta_{22}{=}K_{2,D}^{d} (K_{2,R}^{u})^{*}$, and $\gamma_{id,RD} = P_t |h_{RD}|^2 / \sigma_n^2$ denoting the ideal SNR in the absence of IQI. When the IQI is negligible, we obtain $\vartheta_{11} = 1$, $\vartheta_{12} = 0$, $\vartheta_{21} = 0$ and $\vartheta_{22} = 0$ and finally (5) simplifies to $\gamma_{RF,RD} = \gamma_{id,RD}$.

B. FSO Subsystem

The FSO links of the hybrid system operate with intensity modulation and direct detection (IM/DD) mode [4]. In case that the FSO link is selected at S for transmission towards R, the optical signal is emitted by S and propagates through the atmospheric channel. The received optical signal at R is distorted by the joint effects of atmospheric turbulence and pointing errors [3], [4]. Note that the $S - R$ and $R - D$ FSO links are identical, since no interference occurs at R and no interference takes place between the $S - R$ and $R - D$ received optical beams. Therefore, the received optical signal at the input of the photodetector (PD) at R or D is [17]

$$y_{X,FSO}(t) = I_k s(t) + n_{opt,X}(t), \tag{6}$$

where $s(t)$ is the transmitted optical signal from S or R with average power $\mathbb{E}[|s(t)|^2] = P_0$, I_k, $k \in (SR, RD)$ is the total real-valued instantaneous channel coefficient of each link, and n_{opt} corresponds to the AWGN of the optical link $n_{opt,X} \sim \mathcal{N}(0, \sigma_{n,opt,X}^2)$. The total channel coefficient I_k is equal to $I_k = I_{l,k} I_{t,k} I_{p,k}$, where $I_{l,k}$ represents the deterministic attenuation of the optical signal due to path and power loss, while $I_{t,k}$ and $I_{p,k}$ denote the random variables (RVs) due to atmospheric turbulence and pointing errors, respectively. For simplification, we set $I_{l,k} = 1$ and as a result, I_k becomes $I_k = I_{t,k} I_{p,k}$.

The average electrical SNR at the output of the PD of each individual k-th FSO link is [4]

$$\bar{\gamma}_{FSO,k} = \frac{\left(\rho_k P_0 \mathbb{E}[I_k]\right)^2}{\sigma_{n,opt,X}^2}, \tag{7}$$

with ρ_k being the PD responsivity. As $I_{t,k}$ and $I_{p,k}$ are independent, we obtain $\mathbb{E}[I_k] = \mathbb{E}[I_{t,k}]\mathbb{E}[I_{p,k}]$.

For the atmospheric turbulence effect, the Gamma-Gamma (GG) distribution model is considered in this work, which accurately describes the irradiance fluctuations from weak up to strong turbulence conditions [3]. Along with the turbulence effect, we also consider misalignment fading due to pointing errors. The joint probability distribution function, including both of these effects, is [17]

$$f_{I_k}(I_k) = \frac{a_k b_k \xi_k^2}{A_{0,k} \Gamma(a_k) \Gamma(b_k)} \times G_{1,3}^{3,0}\left(\frac{a_k b_k I_k}{A_{0,k}}\middle| \begin{matrix} \xi_k^2 \\ \xi_k^2 - 1, a_k - 1, b_k - 1 \end{matrix}\right), \tag{8}$$

where $\Gamma(.)$ denotes the gamma function and $G_{p,q}^{m,n}\left(z| \begin{matrix} a_p \\ b_q \end{matrix}\right)$ is the Meijer's G-function [18, Eq. (9.301)]. The parameters a_k, b_k correspond to the GG distribution parameters and describe large and small scale turbulence effects, respectively. Their values are given in [17, Eqs. (8)-(9)] for spherical wave propagation, and are connected to the Rytov variance $\sigma_{R,k}^2$ and the diameter D_k of each RX aperture. The Rytov variance is linked to the link distance L_k of the k-th link, and the refractive index structure parameter C_n^2. The C_n^2 parameter takes values in the range between $10^{-17} - 10^{-13} m^{-2/3}$ for weak up to strong turbulence conditions. Moreover, ξ_k and $A_{0,k}$ are the pointing errors parameters [17], connected with the beam radius on the receiver plane $W_{z,k}$ and the pointing error displacement $\sigma_{s,k}$. The beam radius on the RX plane at distance L_k is calculated as $W_{z,k} = W_k \sqrt{1 + 1.63 \sigma_{R,k}^{12/5} \Lambda_k}$ where $W_k = W_0 \sqrt{\Theta_{0,k}^2 + \Lambda_{0,k}^2}$ with $\Theta_{0,k} = 1 - \frac{L_k}{F_0}$, $\Lambda_{0,k} = \frac{2 L_k}{\kappa W_0}$ and $\Lambda_k = \frac{\Lambda_{0,k}}{\Theta_{0,k}^2 + \Lambda_{0,k}^2}$ with $\kappa = \frac{2\pi}{\lambda}$ the optical wavenumber. The parameter W_0 corresponds to the beam radius at each TX of the FSO links and F_0 is the phase front radius of curvature [3]. Finally, we have $\mathbb{E}[I_{t,k}] = 1$ and $\mathbb{E}[I_{p,k}] = A_{0,k} \xi_k^2 \left(1 + \xi_k^2\right)^{-1}$ [4, Eqs. (14), (23)].

III. Outage Probability Analysis

In this section, we derive the analytical expressions of outage probability for the individual RF and FSO subsystems and for the dual-hop FD DF relay system composed of parallel hybrid RF/FSO links.

Firstly, we focus on the case of the RF subsystem. When the RF link is active for the $S - R$ link, outage occurs if $\gamma_{RF,SR}$ falls below a predefined threshold $\gamma_{th,RF} = 2^{R_{th,RF}} - 1$ with $R_{th,RF}$ being the achievable threshold rate for the RF links in bits per channel use (BPCU). Towards this direction, we provide the following theorem.

Theorem 1. *By considering the IQI at the front-end of R, the outage probability for the $S - R$ RF link is given by*

$$P_{out,RF,SR} = 1 - \left[1 - \frac{\exp\left(\frac{(1+\gamma_{th,RF})\left|K_{2,R}^{d}\right|^2}{\lambda_{RR} B \frac{P_t}{\sigma_n^2}}\right)}{\left(\frac{\left|K_{1,R}^{d}\right|^2}{\gamma_{th,RF}} - \left|K_{2,R}^{d}\right|^2\right) \frac{\lambda_{SR}}{\lambda_{RR} B} + 1}\right] \times \exp\left(-\frac{\gamma_{th,RF}}{\lambda_{SR} \frac{P_t}{\sigma_n^2}}\right), \tag{9}$$

where

$$B = |K_{1,R}^{d} K_{1,R}^{u}|^2 + |K_{2,R}^{d} (K_{2,R}^{u})^{*}|^2$$

$$+ |K_{1,R}^{d} K_{2,R}^{u}|^2 + |K_{2,R}^{d} (K_{1,R}^{u})^*|^2.$$

Proof. See Appendix V-A. □

Next we consider the case of the $R-D$ RF link, which is given by the following theorem.

Theorem 2. *The outage probability for the $R-D$ RF link is*

$$P_{out,RF,RD} = 1 - \exp\left(\frac{-\left(|K_{1,D}^{d}|^2 + |K_{2,D}^{d}|^2\right)}{\frac{\lambda_{RD} P_t}{\sigma_n^2} \left(\frac{|\vartheta_{11}|^2 + |\vartheta_{22}|^2}{\gamma_{th,RF}} - \left(|\vartheta_{12}|^2 + |\vartheta_{21}|^2\right) \right)} \right). \tag{10}$$

Proof. See Appendix V-B. □

Subsequently, we concentrate on the FSO subsystem. The k-th FSO links are identical, since no interference occurs at the relay node or from any other ambient source. Thus, the outage probability of the $S-R$ and $R-D$ FSO links can be evaluated with the cumulative distribution function (CDF) of the instantaneous $\gamma_{FSO,k}$. The CDF of $\gamma_{FSO,k}$, for the case of GG with pointing errors, is given by [8, Eq. (30)], and thus the outage probability for the k-th link is

$$P_{out,FSO,k} = \mathbb{P}\left(\gamma_{FSO,k} \leq \gamma_{th,FSO}\right) = F_{\gamma_{FSO,k}}\left(\gamma_{th,FSO}\right) = \frac{\xi_k^2}{\Gamma(a_k)\Gamma(b_k)} G_{2,4}^{3,1}\left(\frac{a_k b_k \mathbb{E}[I_k]}{A_{0,k}} \sqrt{\frac{\gamma_{th,FSO}}{\bar{\gamma}_{FSO,k}}} \middle| \begin{matrix} 1, \xi_k^2 + 1 \\ \xi_k^2, a_k, b_k, 0 \end{matrix} \right) \tag{11}$$

with $k \in (SR, RD)$ and $\gamma_{th,FSO} = 2^{R_{th,FSO}} - 1$.

Finally, we calculate the overall outage probability for the dual-hop FD hybrid system. In this case, it is [16]

$$P_{out,tot} = P_{out,SR} + (1 - P_{out,SR}) P_{out,RD}, \tag{12}$$

where $P_{out,SR}$ is the outage probability of the $S-R$ link and $P_{out,RD}$ denotes the corresponding outage probability of the $R-D$ link. Based on the hard-switching operation, the outage probability of each individual k-th link, is [1]

$$P_{out,k} = P_{out,RF,k} P_{out,FSO,k}. \tag{13}$$

Therefore, we can deduce that the outage probability of a dual-hop FD system composed of hybrid parallel RF/FSO links with hard-switching operation, can be calculated as

$$\begin{aligned} P_{out,tot} =& P_{out,RF,SR} P_{out,FSO,SR} \\ &+ (1 - P_{out,RF,SR} P_{out,FSO,SR}) \\ &\times P_{out,RF,RD} P_{out,FSO,RD}. \end{aligned} \tag{14}$$

IV. Numerical Results

In this section, we illustrate numerical results based on the derived analytical expressions for the outage probability of the dual-hop FD system with parallel hybrid RF/FSO links. Unless otherwise stated, the parameter values used for the RF and FSO subsystems are as follows; $R_{th,RF} = R_{th,FSO} = 5$ BPCU, $P_t/\sigma_n^2 = 60$ dB, $IRR_{R,D}^{u/d} = 41.2$, 19 dB, $C_n^2 = 5 \times 10^{-14} m^{-2/3}$, $\lambda = 1.55$ um, $W_0 = 4$ cm, $F_0 \to \infty$, $D_k = 10$ cm, $\sigma_{s,k}/D_k = 0.1$. All the presented results are verified by Monte Carlo simulations using 10^6 realizations.

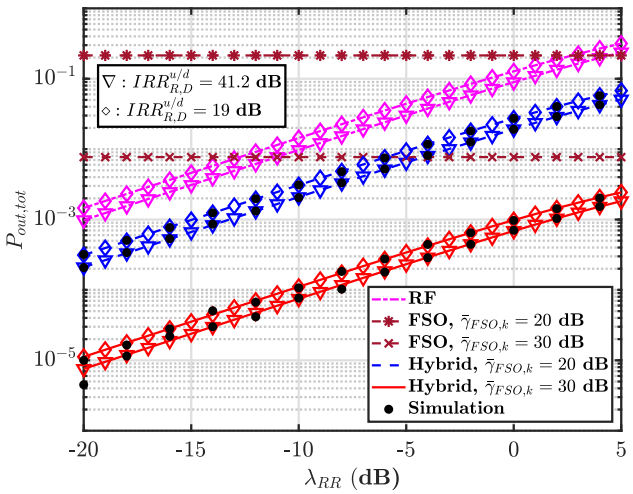

Fig. 2. Outage probability versus λ_{RR}, under the influence of IQI.

Fig. 2 illustrates the outage probability as a function of the mean value of the RSI effect, i.e. λ_{RR}. Moreover, we take into account the IQI impact on the RF subsystem, considering weak and strong IQ mismatches at the RXs and TXs of R and D nodes. For the Rayleigh fading of the RF wireless channels, we set λ_{SR} and λ_{RD}, equal to 25 dB. Under these conditions for the RF links, we assume two cases of operation for the FSO links, with $\bar{\gamma}_{FSO,k} = 20$ dB and 30 dB under strong turbulence conditions. From the illustrated plots, we observe the performance improvement on the outage probability of the dual-hop hybrid system, compared to the case where the dual-hop system consists of exclusively FSO or RF links. As it is shown, an FD RF relaying system achieves outage probability on the order of 10^{-3} for the minimum considered RSI with $\lambda_{RR} = -20$ dB. For higher values of λ_{RR}, the outage probability reaches unacceptable levels. On the other hand, the hybrid system overcomes these limitations. When $\bar{\gamma}_{FSO,k} = 20$ and 30 dB, the outage probability of the hybrid system reaches values below 10^{-3}. For the first case, the outage probability is kept below this limit up to the value of $\lambda_{RR} = -15$ dB. For the second case, with $\bar{\gamma}_{FSO,k} = 30$ dB, the outage probability lies between 10^{-5} to 10^{-3} across the range -20 to 0 dB for λ_{RR}. Therefore, the detrimental impact of increased RSI can be counterbalanced with the employment of an FD relaying hybrid system composed of RF/FSO links under hard-switching operation. Furthermore, we can observe that for a given $\bar{\gamma}_{FSO,k}$, a lower value of $IRR_{R,D}^{u/d}$ results in a higher outage probability.

Fig. 3 demonstrates the dependence of the outage probability of the hybrid system on the ratio P_t/σ_n^2. For the RF channels, two different cases are employed, which are modeled by $\lambda_{SR} = \lambda_{RD} = 15$ dB and 25 dB, respectively. Various RSI cases are also taken into account with $\lambda_{RR} = -15$ and -5 dB for weak and strong influence of the effect. Regarding the FSO links, we assume strong turbulence conditions with fixed $\bar{\gamma}_{FSO,k} = 20$ dB. We can observe that as the ratio $P_t/\sigma_n^2 \to \infty$, the outage probability converges to constant values. Acceptable

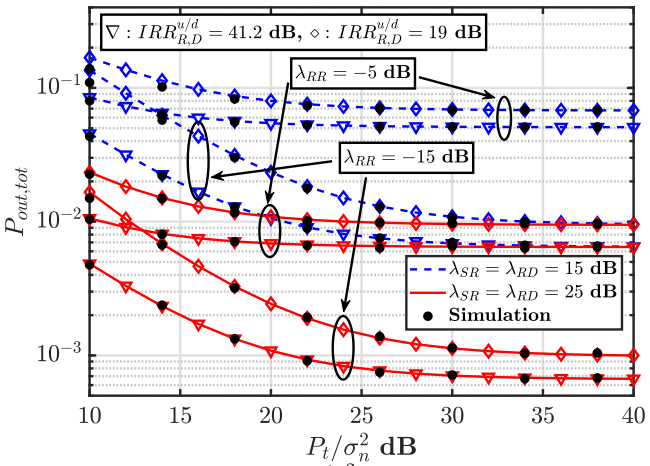

Fig. 3. Outage probability versus P_t/σ_n^2 for different $\lambda_{SR}, \lambda_{RD}$, under the influence of atmospheric turbulence RSI and IQI; $\bar{\gamma}_{FSO,k} = 20$ dB.

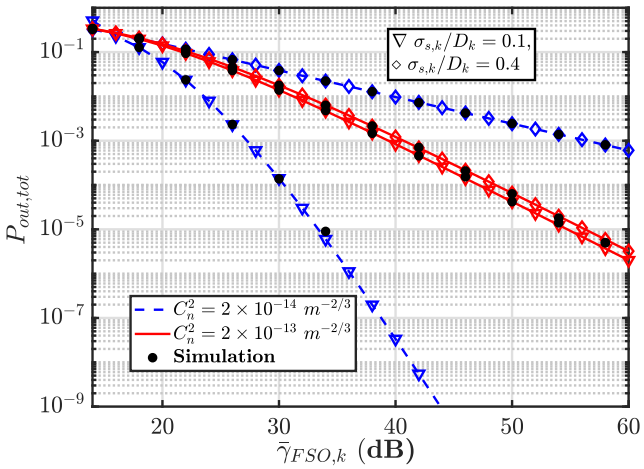

Fig. 4. Outage probability versus $\bar{\gamma}_{FSO,k}$, under moderate and strong influence of atmospheric turbulence and misalignment fading.

performance, below 10^{-3}, is achieved when $\lambda_{SR} = \lambda_{RD} = 25$ dB and $P_t/\sigma_n^2 > 30$ dB. It is worth pointing out the impact of the IQI effect on the dual-hop hybrid system, especially when $P_t/\sigma_n^2 < 25$ dB. Under these conditions, a significant difference, between the two considered cases of $IRR^{u/d}_{R,D}$, occurs. Based on the aforementioned, we can infer that higher availability for the dual-hop FD hybrid RF/FSO system can be achieved with $\bar{\gamma}_{FSO,k} > 20$ dB.

Finally, in Fig. 4, we present outage probability results as a function of the $\bar{\gamma}_{FSO,k}$. For the RF subsystem, we consider $IRR^{u/d}_{R,D} = 25.4$ dB, $\lambda_{SR} = \lambda_{RD} = 10$ dB, and $\lambda_{RR} = -5$ dB. For the FSO links, we assume moderate and strong atmospheric turbulence conditions, with $C_n^2 = 2 \times 10^{-14}$ and 2×10^{-13} $m^{-2/3}$, respectively. Concerning the misalignment fading, we take two values into account for the normalized spatial jitter; $\sigma_{s,k}/D_k = 0.1, 0.4$ corresponding to weak and strong misalignment fading conditions. From the depicted results, we observe the impact of the atmospheric turbulence and pointing errors on the outage probability of the dual-hop FD hybrid system. For moderate turbulence conditions and weak misalignment, the outage probability of the FD relaying hybrid system reaches values below 10^{-3} when $\bar{\gamma}_{FSO,k} \geq 28$ dB. For strong turbulence conditions, we observe that the outage performance between the cases of weak and strong misalignment fading does not differ essentially and $\bar{\gamma}_{FSO,k} \geq 40$ dB is required. However, for moderate turbulence, with $C_n^2 = 2 \times 10^{-14}\ m^{-2/3}$ and $\sigma_{s,k}/D_k = 0.4$, we obtain the worst case performance. This is mainly attributed to the narrow optical beam, where in the case of increased optical beam movement results in increased irradiance fluctuations. For the case of strong atmospheric turbulence, the beam spreading due to turbulence acts in a beneficial way, compensating for the optical beam displacements.

V. Conclusion

In this work, we study a dual-hop FD communication system composed of parallel hybrid RF/FSO links. We take into consideration the RSI and the IQI effects for the RF links, which operate under Rayleigh fading conditions. For the FSO links we assume the influence of the GG atmospheric turbulence in conjunction with the pointing errors effect. The performance of the dual-hop hybrid system is evaluated by the closed-form analytical expressions of outage probability for the dual-hop FD hybrid RF/FSO link. The presented numerical results demonstrate the performance enhancement resulted from the use of parallel hybrid RF/FSO links in a dual-hop FD system. The availability of the whole communication system increases, and the various aggravating effects pertaining to RF and FSO links can be properly overcome.

Appendix

A. Proof of Theorem 1

The $S-R$ SINR, $\gamma_{RF,SR}$, of (4) is a function of the channel gains $|h_{SR}|^2$ and $|h_{RR}|^2$. Firstly, we introduce some approximations for (4). By applying the inequality $|\alpha|^2+|\beta|^2 \gg 2\mathbb{R}(\alpha\beta^*)$, which results in $|\alpha+\beta|^2 \approx |\alpha|^2+|\beta|^2$, we obtain

$$I \approx |K^d_{1,R}K^u_{1,R}h_{RR}|^2 + |K^d_{2,R}(K^u_{2,R}h_{RR})^*|^2 + |K^d_{1,R}K^u_{2,R}h_{RR}|^2 + |K^d_{2,R}(K^u_{1,R}h_{RR})^*|^2 = B|h_{RR}|^2,$$

where the parameter B is presented in Theorem 1. Consequently, we require the conditional probability $\mathbb{P}\left(\gamma_{RF,SR} \leq \gamma_{th} \middle| |h_{SR}|^2\right)$, which is obtained by substitution for the $\gamma_{RF,SR}$ from (4). Since $h_{RR} \sim \mathcal{CN}(0, \sigma^2_{RR})$, the channel gain $|h_{RR}|^2$ is exponentially distributed with mean value λ_{RR}, i.e $f_{|h_{RR}|^2}(x) = \frac{1}{\lambda_{RR}} \exp\left(-\frac{x}{\lambda_{RR}}\right)$ and hence, the conditional probability $\mathbb{P}\left(\gamma_{RF,SR} \leq \gamma_{th} \middle| |h_{SR}|^2\right)$ is obtained as expressed in (15). As a result, the outage probability of the $S-R$ RF link is

$$P_{out,RF,SR} = \int_0^\infty \mathbb{P}\left(\left(\frac{|K^d_{1,R}|^2}{\gamma_{th}B} - \frac{|K^d_{2,R}|^2}{B}\right)x - \frac{\left(|K^d_{1,R}|^2 + |K^d_{2,R}|^2\right)}{B\frac{P_t}{\sigma_n^2}} \leq |h_{RR}|^2 \middle| |h_{SR}|^2\right) f_{|h_{SR}|^2}(x)dx$$

$$\mathbb{P}\left(\gamma_{RF,SR} \leq \gamma_{th} \middle| |h_{SR}|^2\right)$$
$$= \mathbb{P}\left(\left(\frac{\left|K_{1,R}^d\right|^2}{\gamma_{th}B} - \frac{\left|K_{2,R}^d\right|^2}{B}\right)|h_{SR}|^2 - \frac{\left(\left|K_{1,R}^d\right|^2 + \left|K_{2,R}^d\right|^2\right)}{B\frac{P_t}{\sigma_n^2}} \leq |h_{RR}|^2 \middle| |h_{SR}|^2\right),$$
$$= \begin{cases} \exp\left(-\left(\left(\frac{\left|K_{1,R}^d\right|^2}{\gamma_{th}B} - \frac{\left|K_{2,R}^d\right|^2}{B}\right)|h_{SR}|^2 - \frac{\left(\left|K_{1,R}^d\right|^2 + \left|K_{2,R}^d\right|^2\right)}{B\frac{P_t}{\sigma_n^2}}\right) \Big/ \lambda_{RR}\right), & |h_{SR}|^2 > \gamma_{th}/\frac{P_t}{\sigma_n^2}, \\ 1, & |h_{SR}|^2 \leq \gamma_{th}/\frac{P_t}{\sigma_n^2}. \end{cases} \quad (15)$$

$$= \int_0^{\gamma_{th}/\frac{P_t}{\sigma_n^2}} \frac{1}{\lambda_{SR}} \exp\left(-\frac{x}{\lambda_{SR}}\right) dx$$
$$+ \int_{\gamma_{th}/\frac{P_t}{\sigma_n^2}}^{\infty} \exp\left(-\left(\left(\frac{\left|K_{1,R}^d\right|^2}{\gamma_{th}B} - \frac{\left|K_{2,R}^d\right|^2}{B}\right)x - \frac{\left(\left|K_{1,R}^d\right|^2 + \left|K_{2,R}^d\right|^2\right)}{B\frac{P_t}{\sigma_n^2}}\right) \Big/ \lambda_{RR}\right) \frac{1}{\lambda_{SR}} \exp\left(-\frac{x}{\lambda_{SR}}\right) dx$$
$$= 1 - \left[1 - \frac{\exp\left(\frac{(1+\gamma_{th})\left|K_{2,R}^d\right|^2}{\lambda_{RR}B\frac{P_t}{\sigma_n^2}}\right)}{\left(\frac{\left|K_{1,R}^d\right|^2}{\gamma_{th}} - \left|K_{2,R}^d\right|^2\right)\frac{\lambda_{SR}}{\lambda_{RR}B} + 1}\right] \exp\left(\frac{-\gamma_{th}}{\lambda_{SR}\frac{P_t}{\sigma_n^2}}\right). \quad (16)$$

B. Proof of Theorem 2

The outage probability of the $R-D$ RF link, $P_{out,RF,RD} = \mathbb{P}\left(\gamma_{RF,RD} \leq \gamma_{th}\right)$, using (5), is expressed as

$$P_{out,RF,RD} = \mathbb{P}\left(\frac{|K_{1,D}^d|^2 + |K_{2,D}^d|^2}{\frac{|\vartheta_{11}|^2+|\vartheta_{22}|^2}{\gamma_{th}} - (|\vartheta_{12}|^2 + |\vartheta_{21}|^2)} \geq \gamma_{id,RD}\right). \quad (17)$$

In order to calculate the $P_{out,RF,RD}$, the CDF of $\gamma_{id,RD}$ is required. Knowing that $\gamma_{id,RD}$ is a function of $|h_{RD}|^2$, its corresponding CDF is $F_{\gamma_{id,RD}}(x) = 1 - \exp\left(-\frac{x}{\lambda_{RD}\frac{P_t}{\sigma_n^2}}\right)$. Hence, the outage probability for the $R-D$ RF link is

$$P_{out,RF,RD} = F_{\gamma_{id,RD}}\left(\frac{|K_{1,D}^d|^2 + |K_{2,D}^d|^2}{\frac{|\vartheta_{11}|^2+|\vartheta_{22}|^2}{\gamma_{th}} - (|\vartheta_{12}|^2 + |\vartheta_{21}|^2)}\right)$$
$$= 1 - \exp\left(\frac{-\left(|K_{1,D}^d|^2 + |K_{2,D}^d|^2\right)}{\frac{\lambda_{RD}P_t}{\sigma_n^2}\left(\frac{|\vartheta_{11}|^2+|\vartheta_{22}|^2}{\gamma_{th}} - (|\vartheta_{12}|^2 + |\vartheta_{21}|^2)\right)}\right). \quad (18)$$

ACKNOWLEDGMENT

This work was co-funded by the European Regional Development Fund and the Republic of Cyprus through the Research and Innovation Foundation, under the projects EXCELLENCE/0918/0377 (PRIME) and INFRASTRUCTURES/1216/0017 (IRIDA).

REFERENCES

[1] M. Usman, H. Yang, and M.-S. Alouini, "Practical switching-based hybrid FSO/RF transmission and its performance analysis," *IEEE Photonics J.*, vol. 6, no. 5, pp. 1–13, Oct. 2014.

[2] I. I. Kim and E. J. Korevaar, "Availability of free-space optics (FSO) and hybrid FSO/RF systems," in *Optical Wireless Communications IV*, vol. 4530. Denver, CO, US: SPIE, Nov. 2001.

[3] L. C. Andrews and R. L. Phillips, *Laser Beam Propagation through Random Media*. Bellingham, WA, US: SPIE, 2005.

[4] H. AlQuwaiee, H.-C. Yang, and M.-S. Alouini, "On the asymptotic capacity of dual-aperture FSO systems with generalized pointing error model," *IEEE Trans. Wirel. Commun.*, vol. 15, no. 9, pp. 6502–6512, Sep. 2016.

[5] I. Krikidis, H. A. Suraweera, P. J. Smith, and C. Yuen, "Full-duplex relay selection for amplify-and-forward cooperative networks," *IEEE Trans. Wirel. Commun.*, vol. 11, no. 12, pp. 4381–4393, Dec. 2012.

[6] D. Bharadia, E. McMilin, and S. Katti, "Full duplex radios," in *Proc. ACM SIGCOMM 2013*, Hong Kong, China, Aug. 2013.

[7] D. Korpi, S. Venkatasubramanian, T. Riihonen, L. Anttila, S. Otewa, C. Icheln, K. Haneda, S. Tretyakov, M. Valkama, and R. Wichman, "Advanced self-interference cancellation and multiantenna techniques for full-duplex radios," in *Proc. 46th Asilomar Conf. Signals, Syst. Comput.*, Pacific Grove, CA, Nov. 2013.

[8] H. E. Nistazakis, M. P. Ninos, A. D. Tsigopoulos, D. A. Zervos, and G. S. Tombras, "Performance study of terrestrial multi-hop OFDM FSO communication systems with pointing errors over turbulence channels," *J. Mod. Opt.*, vol. 63, no. 14, pp. 1403–1413, June 2016.

[9] T. Riihonen, S. Werner, and R. Wichman, "Comparison of full-duplex and half-duplex modes with a fixed amplify-and-forward relay," in *IEEE Wirel. Commun. Netw. Conf.*, Budapest, Hungary, Apr. 2009.

[10] L. Anttila, M. Valkama, and M. Renfors, "Circularity-based I/Q imbalance compensation in wideband direct-conversion receivers," *IEEE Trans. Veh. Technol.*, vol. 57, no. 4, pp. 2099–2113, July 2008.

[11] A. A. Boulogeorgos, P. C. Sofotasios, B. Selim, S. Muhaidat, G. K. Karagiannidis, and M. Valkama, "Effects of RF impairments in communications over cascaded fading channels," *IEEE Trans. Veh. Technol.*, vol. 65, no. 11, pp. 8878–8894, Nov. 2016.

[12] M. Najafi, V. Jamali, and R. Schober, "Optimal relay selection for the parallel hybrid RF/FSO relay channel: Non-buffer-aided and buffer-aided designs," *IEEE Trans. Commun.*, vol. 65, no. 7, pp. 2794–2810, July 2017.

[13] S. Sharma, A. S. Madhukumar, and R. Swaminathan, "Switching-based cooperative decode-and-forward relaying for hybrid FSO/RF networks," *IEEE/OSA J. Opt. Commun. Netw.*, vol. 11, no. 6, pp. 267–281, Jun. 2019.

[14] G. D. Roumelas, H. E. Nistazakis, E. Leitgeb, H. D. Ivanov, C. K. Volos, and G. S. Tombras, "Serially DF relayed hybrid FSO/MMW links with Weibull fading, $\mathcal{M}$-turbulence and pointing errors," *Optik*, vol. 216, p. 164531, Aug. 2020.

[15] M. K. Simon and M.-S. Alouini, *Digital Communication over Fading Channels*, 2nd ed. New York, NY, US: Wiley-IEEE Press, 2005.

[16] M. Mokhtar, N. Al-Dhahir, and R. Hamila, "OFDM full-duplex DF relaying under I/Q imbalance and loopback self-interference," *IEEE Trans. Veh. Technol.*, vol. 65, no. 8, pp. 6737–6741, Aug. 2016.

[17] K. P. Peppas, A. N. Stassinakis, H. E. Nistazakis, and G. S. Tombras, "Capacity analysis of dual amplify-and-forward relayed free-space optical communication systems over turbulence channels with pointing errors," *IEEE/OSA J. Opt. Commun. Netw.*, vol. 5, no. 9, pp. 1032–1042, Sep. 2013.

[18] I. S. Gradshteyn and I. M. Ryzhik, *Table of Integrals, Series, and Products*, 7th ed. Burlington, MA, US: Elsevier, 2007.